Identification of SPINT3 as a metastatic suppressor in gastric cancer through induction of TGF-β1 secretion

Haifeng Wang
Zhejiang University
Haohao Wang
Zhejiang University
Teng Li-song (lsteng@zju.edu.cn)
Zhejiang University

Research Article

Keywords: SPINT3 (serine peptidase inhibitor, Kunitz type, 3), gastric cancer, TGF-β1 secretion, tumor metastasis

Posted Date: May 11th, 2022

DOI: https://doi.org/10.21203/rs.3.rs-745710/v2

Abstract

Background

Cancer metastasis is responsible for most cancer-related deaths. *SPINT3* (serine peptidase inhibitor, Kunitz type, 3) is a newly identified gene, and its relationship with gastric cancer has not been well studied.

Methods

We first designed an sgRNA sub-library to screen for metastatic suppressors, and chose *SPINT3*. We then used QPCR and western blotting to detect the expression level of SPINT3 in gastric cancer tumor tissues. In addition, we used annexin V/propidium iodide (PI) to detect changes in apoptosis. PI staining and wound healing assays were used to detect the cell cycle and changes in cell migration, respectively. Finally, CyTOF and T cell proliferation experiments were performed to detect changes in immune cells in the tumor microenvironment.

Results

sgRNA which target the *SPINT3* gene was present in every metastatic tumor. The expression of *SPINT3* was low in gastric cancer tissues, and this increased the metastatic ability of gastric cancer cells. In addition, high expression of *SPINT3* induced cell apoptosis, downregulated cell proliferation, and impaired cell migration. Furthermore, low expression of *SPINT3* induced the secretion of TGF-β1 and an immunosuppressive signal, which could be blocked by Apatinib and SB431542.

Conclusion

We confirmed that *SPINT3* is a metastasis suppressor in gastric cancer.

1. Introduction

Gastric cancer is the fifth most common cancer in the world after lung, breast, colorectal, and prostate cancer [1]. In 2012, there were approximately 952,000 new cases and 723,000 gastric cancer-related deaths worldwide [2]. Gastric cancer is characterized by geographical distribution, and is common in East Asia, Central Europe, and South America [3]. The number of gastric cancer-related deaths in China in 2012 was 320,000, accounting for 45% of total deaths in the country [4]. This shows that the disease burden of gastric cancer is extremely heavy, and it makes the search for new biomarkers and therapeutic targets a top priority.

TGF-β1(Transforming growth factor beta 1) is a critical factor in gastric cancer metastasis [5], previously studies already showed that TGF-β increased in the serum, gastric mucosa and precancerous gastric cells [6], in the meantime, elevated TGF-β also correlated with lymph node metastasis and survival rate of gastric cancer patients [7]. Thus, knowing the regulation of TGF-β1 become critical.

Recently studies already showed that the secretion of TGF-β1 in the tumor microenvironment (TME) could significantly induce the immune suppression signal, which further promote the proliferation and invasion of tumor [8]. So in this study, we firstly using sub-library to screen the TGF-β1 binding genes to find out the gene responsible for the TGF-β1 secretion as well as the modification of TME. *SPINT3* is a relatively new gene, which firstly identified in 2011, it transcript of 476 bp and will be processed to a secreted protein of 7.6 kDa, and its function might be related to serine-type endopeptidase inhibitor activity, receptor antagonist activity and transforming growth factor beta binding [9], however, the relation between SPINT3 and gastric cancer remain unclear. We chose *SPINT3* as our candidate gene owing to the wide presence of *SPINT3* sgRNA in a metastatic mouse model. Studies have shown that *SPINT3* is expressed at low levels in gastric cancer tissues, and that downregulation of *SPINT3* activates tumor cell metastasis and generates an immunosuppressive signal.

2. Materials And Methods

2.1 Ethics Statement

This the study was carried out in compliance with the ARRIVE guidelines. All experiments were approved by the First Affiliated Hospital of Zhejiang University. All the patients involved in this study provided informed consent, and all the sample extraction protocols followed the Declaration of Helsinki and were authorized by the Institutional Ethics Board of The First Affiliated Hospital, School of Medicine, Zhejiang University. All mouse experiments were performed at the First Affiliated Hospital of Zhejiang University in accordance with the relevant guidelines and regulations formulated by the hospital. Mice were anesthetized using avertin and sacrificed by applying excessive carbon dioxide.

2.2 Patient samples

Tumor tissues and adjacent normal tissues of five cases of gastric adenocarcinoma were collected from The First Affiliated Hospital, School of Medicine, Zhejiang University. The samples were divided into two parts and subjected to QPCR and western blotting, depending on the size of the sample.

2.3 Sub-library design, preparation and infection

(1) Twenty-two genes belonging to GO:0050431 were selected, and the sgRNA that target these genes were designed, each gene was allocated with 3 sgRNAs; the sgRNA oligo sequences are listed in Table 1. (2) Oligos were cloned into the lentiCRISPR v2 vector (Addgene 52961) backbone. (3) The vectors were packaged as lentiviruses using the 2nd lentivirus package system: Firstly the concentration of library vector was quantified by A260nm/A280nm, mixed with the genome vector and package vector of lentivirus, ratio is target vector: psPAX2(Addgene 52960):pMD2.G(Addgene 52959) = 4:3:1, then the vector

was transfected into 293t cell lines, after 48 h of transfection, supernatant of culture medium was collected and using single clone experiment to measure the titer of virus.

2.4 Cell culture, generation of different phenotype of cells and drug treatment

(1) Cell culture: Human gastric cancer cell line MKN-45 and mouse gastric cancer cell line MFC were used in this study, MKN-45 cells was cultured in DMEM + 10%FBS, MFC cells were cultured in RPMI1640 + 10%FBS, culture condition is 37 ℃, 5% CO2. (2) Generation of Sub-library cells: Before the infection of library virus, MKN-45 cells were label with GFP by infection of GFP virus, package of lenti virus followed 2.5 part, target vector of GFP virus is pCDH-EF1α-MCS-T2A-GFP (SYSTEM BIOSCIENCES(SBI) CD526A-1). the MKN-45 cells was then infected with sub-library virus in a MOI of 0.1 to ensure 1 cell been infected by 1 lentivirus, after selected by 4ug/mL puromycin for 7 days, MKN-45 library cells were utilized to subsequent experiment. (3) Generation of SPINT3 related phenotype: For the in vivo study, MKN-45 cells and MFC cells were first labeled with GFP as previously described, cells used in the in vitro study does not involve the GFP to prevent the interference from GFP protein. MKN-45 and MFC cells were first divided into CON, SPINT3 overexpression, SPINT3 sgRNA and SPINT3 shRNA group, then for the in vivo study, cells were infected with CON (lentiCRISPR v2 backbone), SPINT3 overexpression virus, SPINT3 sgRNA virus and SPINT3 shRNA virus, for the in vitro study, cells were also transfected with the coordinated vector. (4) Drug treatment: Apatinib(S5248) and SB431542(S1067) were all purchased from Selleckchem company. For in vitro treatment, cells were treated with 25 uM of Apatinib or 1 uM of SB431542 for 72 h. For in vivo treatment, mice were injected with 50 mg/kg of Apatinib or 100 uL of SB431542 (1uM solution) after 3 days of injection of tumor cells, method of injection is intraperitoneal, and every mice were injected with 2 times a week.

2.5 Mouse experiment

The SCID, nude, and 615 mice used in this study were housed in the animal facility of the First Affiliated Hospital of Zhejiang University. (1) For the library experiment, nude mice (6–8 weeks old) were injected subcutaneously with the CON or *SPINT3* -shRNA MKN-45 cell line, and then the primary tumors were harvested, cut into 1 mm × 1 mm × 1 mm slices, and implanted in the gastric mucosa of SCID mice. (2) To detect the tumor microenvironment, 5 million CON or *Spint3*-shRNA MFC cells were injected subcutaneously into 615 mice; after 2 weeks, the primary tumors were harvested and digested into single cells. For, Mice were anesthesia by avertin in the implantation of tumor cells, and sacrificed by excessive carbon dioxide inhalation. To quantify the GFP intensity in fluorescent field, image were first transformed to 16-bit gray scale image, then the total image was selected, and calculate the gray value of whole image by image J software, the GFP intensity ratio was quantified by the ratio of (gray value in other group)/(gray value in CON group).

2.6 In silico analysis

In this study, all in silico analyses were completed using R 3.4.3 software. (1) Extraction of 22-gene list: the transforming growth factor beta binding pathway (GO:0050431) was selected, and the genes involved

in this pathway were extracted using AnnotationDbi and annotated using the org.Hs.eg.db package. (2) Other analysis: TCGA-STAD (Stomach adenocarcinoma dataset from The Cancer Genome Atlas Program) data were downloaded and normalized using the GDCRNATools package, and the gene expression data, follow-up time, and survival status of patients were extracted and analyzed using the univariate COX algorithm. For pathway enrichment analysis, samples were first divided into *SPINT3* low and high expression groups based on the expression of *SPINT3*; then, the GSEA function from the clusterProfile package was used to detect pathway enrichment in *SPINT3* low expression samples and compare it with that in *SPINT3* high expression samples.

2.7 QRT-PCR

(1) Firstly, cells were lysed with 500 μL TRIzol and centrifuged at 12000 rpm for 10 min to remove the cell fraction. (2) The solution was added to 200 μL chloroform, shaken up and down for 15 s, and centrifuged at 12000 rpm for 15 min. (3) 100 μL of the supernatant was drawn, mixed with 100 μL isopropanol, and centrifuged at 12000 rpm for 10 min. (4) The precipitate was washed with 75% ethanol, and the concentration of total RNA was detected using the OD at 260 nm/280 nm. (5) Total mRNA was reverse transcribed using the PrimeScript RT Reagent Kit with gDNA Eraser (R047A, Takara Bio) and TB Green Premix Ex Taq (Tli RNase H Plus) (RR420A, Takara Bio) to detect the expression of the internal reference gene and target gene; the primer sequences used in this study were human *SPINT3* F-5'-GATCTCCTCCCAAATGTATGCGC-3', R-5'-TCCGCAGCCTCCGTAAGCAAAT-3', and human *SPINT3* F-5'-GTCTCCTCTGACTTCAACAGCG-3', R-5'-ACCACCCTGTTGCTGTAGCCAA-3'. The expression level of SPINT3 was determined using the $2^{-\triangle\triangle CT}$ value, then the relatively expression of SPINT3 is quantified by the fold change of ($2^{-\triangle\triangle CT}$ value of target group)/($2^{-\triangle\triangle CT}$ value of control group).

2.8 Western blotting

(1) Bulk tissue was lysed using RIPA buffer on ice for 30 min, mixed with loading buffer, and boiled for 15 min. (2) 20ug of samples were loaded on polyacrylamide gels and proteins were separated based on molecular weight using electrophoresis. (3) The proteins were then transferred to a PVDF membrane and blocked with 5% BSA solution. (4) To save the antibodies, PVDF membrane was cropped before hybridization with antibodies .(5) the membrane was labeled with different primary antibodies, including GAPDH (ab8245), TGF-β1 (ab215715), TGF-β type 1 receptor (ab31013), TGF-β type 2 receptor (ab186838), Smad3 (ab40854), and p-Smad3 (ab52903), PI3K gama(ab154598), PI3K-p85(ab191606), p-AKT1(Ser473) (ab81283), p-MEK1(ab96379), t-GSK3β (ab93926), β-catenin(ab32572) which were all purchased from Abcam. t-MEK1(12761), p-GSK3β(Ser9) (9322), p-β-catenin(Ser 33,37)(9651), p-ERK1/2(4370), t-ERK1/2(4695) were purchased from Cell Signaling Technology. The SPINT3 antibody was synthesized by Beyotime Company (Shanghai, China), dilution is 1:1000. After culturing overnight, the membrane was washed thrice and labeled with secondary antibodies, and protein expression was quantified using ECL solution. To quantify the expression of genes in protein level, plots of gel were first transformed to 16-bit gray scale image, then calculate the gray value of target band by image J software. Finally, the relative expression of gene was revealed by the fold change of CON group.

2.9 Cell apoptosis, proliferation, migration, and cell cycle

For cell apoptosis, proliferation, and cell cycle experiments, MKN-45 cells were first transfected with the CON and *SPINT3* overexpression vectors for 48 h. (1) Cell apoptosis was detected using the APC-conjugated Annexin-V/propidium iodide (PI) kit (BD Biosciences, San Jose, CA, USA). Cells were firstly harvested and washed with PBS, and then suspended in annexin V binding buffer; 5 μL of annexin V APC antibody and 5 μL of PI were added, and after culturing for 15 min, the BD Calibur machine was used to detect positive cells from the FL2 and FL4 channels. The ratio of apoptotic cells was quantified using the percentage of APC-positive cells. (2) Cell proliferation was detected using Cell Counting Kit-8 (CCK-8) (Dojindo Molecular Technologies, Rockville, MD, USA); firstly, cells were dispersed in a 96-well plate, each well was seeded with 2000 cells, 10 μL of CCK-8 solution was added, and the cells were cultured for 2 h. Then, a microplate reader was used to measure the OD at 450 nm, and the proliferation index was quantified using the ratio OD450 nm at other time point/OD450 nm at 0 h. After took the picture, distance of migration in CON and *SPINT3* group were quantified by ruler, and divided it timing, fold change of the migration velocity equals to (migration velocity in other group)/ (migration velocity in CON group). (3) Cell migration: Cells were firstly dispersed in a 24-well plate, and each plate was seeded with 100000 cells; after cell attachment, white tips were used to scratch the bottom, and pictures were taken at the 0 and 12 h time points. (4) Cell cycle: After transfection of the SPINT3 vector for 48 h, cells were washed with PBS and fixed in 70% ethanol overnight. The cells were then stained with PI and cultured for 20 min; the BD Calibur machine was used to detect changes in the cell cycle.

2.10 CyTOF experiment

(1) Firstly, single cells from primary tumors were isolated and the CyTOF experiment was completed by Novogene (Beijing, China). The markers used in CyTOF analysis included LY6G, CD8A, CD45, CD11B, CD28, CD3E, LY6C, CD19, CD24, CD14, F4-80, and CD326. (2) After obtaining the FCS file, the data were analyzed using R 4.0.2 software. The FCS file was read using the flowCore package, and analyzed using the Rtsne package; the conditions used for the Rtsne function were tsne_expr, check_duplicates = FALSE, pca = T,pca_scale = T,perplexity = 120. Finally, the results were visualized using the ggplot2 package.

2.11 T cell proliferation

2.11.1 Isolation of myeloid-derived suppressor cells (MDSCs) and T cells

(1) Firstly, the spleen was ground and washed off with PBS, and then red blood cells were lysed and filtered with a 40 μm filter. (2) Simultaneously, the primary tumor was washed with PBS and lysed with red blood cells. (3) The single-cell suspension of the primary tumor was treated with CD11b and GR1 antibodies, and then with CD3, CD4, and CD8 antibodies. After 30 min of ice labeling, PBS was used for washing. (4) CD11b + GR1 + cells were isolated from bone marrow single-cell suspensions using a BD aria III sorting instrument, and CD3 + CD4- CD8 + T cells were obtained from the spleen single-cell suspension.

2.11.2 Detection of T cell proliferation

(1) CFSE was added to the T cell suspension. After labeling, the cells were washed with PBS. (2) The labeled T cells were divided into two parts. One part was used to detect the expression of CFSE by flow cytometry, and the other part was used for co-culture with MDSCs. (3) After counting the MDSC cell suspension, the supernatant of the CoN group or SPINT3 sgRNA group was used for re-suspension, and 2 folds of CD8 + T cells were added. (4) CFSE expression in CD11b- cells was detected using flow cytometry. Cells with a lower fluorescence intensity at 0 h were used as T cells in the proliferation phase.

2.12 ELISA (enzyme-linked immunosorbent assay)

Total TGF-β1 and active form of TGF-β1 in the supernatant of culture cells was detected by ELISA, ELISA kit for total TGF-β1 detection(436707) and free active of TGF-β1 detection(437707) were all purchased from BioLegend company. Experiment was finished by the assay procedure provided by BioLegend company. (1) Diluting top standard(500 pg/mL) with Assay Buffer C to Prepare different concentration of TGF-β1 solution, which been used to construct the standard curve. (2) Washing plate with Wash Buffer and add 50 uL of Assay Buffer C to each well. (3) Add 50 uL of standard TGF-β1 solution or samples to each well, then seal the plate and incubate in room temperature for 2 h. (4) Wash the plate and add 100 uL of TGF-β1 antibody, incubate for 1 h. (5) Wash the plate and add 100 uL of Avidin-HRP solution, seal the plate and incubate for 30 min. (6) Wash the plate and add 100 uL of Substrate Solution F, incubate for 10 min. (7) Add 100 uL of Stop Solution, read the plate with Microplate Readers at the absorbance of 570 nm, and the concentration of TGF-β1 was quantified by standard curve.

2.13 Statistical analysis

The significance levels in this study were determined using the Student's t-test: $*P < 0.05$, $**P < 0.01$, $***P < 0.001$.

3. Results

3.1 Identification of *SPINT3* as a possible metastatic suppressor by using CRISPR knock out sub-library

TGF-β1 is initially consisted of ~50-kDa pro-protein containing growth factor, LAP and TGF-β binding protein such as LTBP1(latent transforming growth factor β binding proteins 1), LTBP2 [10]. Once the TGF-β1 binding protein is deficient, secretion of TGF-β1 would be highly increased, which would further induce the tumor growth and metastasis [11].

In light of the important role of TGF-β binding protein in cancer, we first extracted 22 genes from the transforming growth factor beta binding pathway (GO:0050431), and then synthesized an sgRNA library

to target these 22 genes, as shown in Fig. 1A. After 12 weeks, all the SCID mice were dissected, and the presence of the GFP signal was detected. Among the 20 SCID mice implanted with gastric cancer tissue from the sgRNA library group, 12 developed lung metastasis, and the other 8 SCID mice implanted with MKN-45 primary tumor tissue did not have any metastatic tumors, suggesting that some of the driver gene in metastasis was knock out in those 12 mice(Fig. 1B). We harvested the lung tissue from those 12 metastatic library mice, and extract the genome DNA, then amplified by the sgRNAs specific primers as descripted in the methods 2.5 part, we confirmed that *SPINT3* sgRNA showed up in every mice belong to the metastatic library mice (Fig. 1C) other than the non-metastatic library mice (Fig. 1G). also for the other 21 genes, *VASN* sgRNA was present in 6 mice from metastatic library mice, and *TWSG1* sgRNAs was present in 5 mice from metastatic library mice (Fig. 1C, D). *VASN* gene is tumor related gene which already been studied. In lung cancer, *VASN* is a potential lung cancer–promoting factor, overexpression of VASN could promote the bronchial epithelial cell transformation through autophagy-mediated apoptosis [12]. In glioma cancer, *VASN* is responsible for the maintenance of glioma stem-like cells through the regulation of NOTCH1 signaling [13], as to gastric cancer, it's already been studied in a PhD thesis even it's not been published (DOI:10.27232/d.cnki.gnchu.2021.000019). And the relation between *TWSG1* and gastric cancer already been proved, TWSG1 could bound to BMP4 and inhibited BMP4-binding activity to BMPR-II [14], it could also been a target of miR-593-5p, and further modulate the proliferation of gastric cancer cell in vivo and in vitro [15]. Thus we preliminary chose *SPINT3* for further investigation due to the high frequency of *SPINT3* sgRNA in metastatic tissue, also to avoid the conflicts with existing research.

As to the other 8 non-metastatic mice, they were sacrificed at the same time to verify the metastasis. Unlike the clinical situation, which the most common sites of metastasis in gastric cancer patients were liver and peritoneum, the liver of all the metastatic library mice were normal (Fig. 1E), in the meantime, all the sgRNAs target 22 genes such as *SPINT3* did not showed up in the liver and peritoneum tissue of metastatic library mice (Fig. 1F), suggesting the mouse model we developed mainly focus on the lung metastasis. Furthermore, by using QPCR, we proved that the expression of *SPINT3* in mRNA level is lower in gastric cancer tissue, lung metastatic tissue from metastatic library mice compared with non-metastatic mice, which indicated that the *SPINT3* low expression cell had highly metastasis ability (Fig. 1H). Based on these results, we chose *SPINT3* as our candidate gene for further analysis.

3.2 Deficiency of *SPINT3* increased lung metastasis of gastric cancer cell line

According to the literature, the function of SPINT3 includes serine-type endopeptidase inhibitor activity [9]; however, the exact role of *SPINT3* in gastric cancer remains unknown. Hence, we first downloaded the gastric cancer dataset from the TCGA database, there are 35 healthy donor tissue and 415 gastric cancer tissue included in this dataset, we then extract the RSEM value of *SPINT3* and normalized by log2 transformation, and confirmed that expression *SPINT3* in these 2 groups were 9.51 ± 3.16 vs 4.38 ± 2.19, using 2-tailed t-test, we confirmed that *SPINT3* expression was significantly lower in gastric cancer tissue than in healthy tissue ($P < 0.05$) (Fig. 2A). We also detect the expression of *SPINT3* in 5 pairs of tumor adjacent tissue and gastric cancer tissue, and confirmed that the expression *SPINT3* in mRNA level is

1.09 ± 0.23 vs 0.31 ± 0.16, *P* value is lower than 0.0001(Fig. 2B). Among these 5 pairs of tissue, we selected 3 pairs as there was not enough tissue in the other 2 pairs. By using western blot, we also proved the consistently low expression of SPINT3 in stomach tumor tissue (Fig. 2C). From a clinical perspective, TCGA-STAD dataset were divided into *SPINT3* low and *SPINT3* high group based on the median of RSEM value of *SPINT3*, then using univariate COX to assess the difference of overall survival rate, patients with low *SPINT3* expression would have a poorer prognosis, P value lower than 0.05, and HR (95% CI for HR) is 0.82(0.59–0.96), suggesting that SPINT3 is a possible tumor suppressor in gastric cancer (Fig. 2D).

To further validate the role of *SPINT3* in gastric cancer, we then chose gastric cancer cell line MKN-45 and MFC. For the MFC cell line, it's also been called as CVCL_5J48 and derived from 615 mice, similar to the mouse model we developed in Fig. 1A, MFC cells prone to blood-born metastasis to lung in 615 mice, better yet the immune system of 615 mice is normal compared with SCID and nude mice, which perfectly for the subsequently experiment. Given that *SPINT3* was consistently expressed at low levels in gastric cancer tissue, we next inhibited *SPINT3* by using shRNA and sgRNA approach. Firstly, we set up the MKN-45 CON, MKN-45 *SPINT3* sgRNA, MKN-45 *SPINT3* shRNA, MFC CON, MFC *Spint3* sgRNA, MFC Spint3 shRNA phenotype, and transfected with CON vector (Lenti V2 vector), human *SPINT3* sgRNA, human *SPITN3* shRNA, mouse *Spint3* sgRNA, mouse *Spint3* shRNA for 48h, and using western blot to check the expression of SPINT3 in protein level. (Fig. 2E). By using the mouse model developed in Fig. 1A, lung metastasis nodules in *SPINT3* sgRNA group was significantly increased compared with the CON group (Fig. 2F) (*n* = 6 mice/group). We then transformed the fluorescent image to gray scale image, and using Image J software to calculate the change of gray value in CON and *SPINT3* KO group, results showed that GFP intensity in *SPINT3* sgRNA group was highly increased (Fig. 2G). In addition, lung metastatic tumor tissue from 2 groups were harvested, and using western blot, we detected decreased *SPINT3* expression in the lung metastasis nodules (Fig. 2H), proving the link between low expression of *SPINT3* and increased lung metastasis.

3.3 Relation between expression of SPINT3 and biological characteristics of gastric cancer cell.

We then designed human and mouse SPINT3 overexpression vector, and transfected it into these 2 gastric cancer lines. Using western blot, we confirmed that the level of SPINT3 expression was elevated in the *SPINT3* cDNA-transfected MKN-45 (Fig. 3A upper panel) and MFC (Fig. 3A lower panel). Using Annexin V/PI double staining, we found that apoptosis was induced after transfection of *SPINT3* cDNA for 48 h (Fig. 3B), in this process, cleaved caspase 3 was increased, suggesting that the *SPINT3* induced apoptosis is caspase dependent (Fig. 3C); moreover, cell proliferation of *SPINT3*-overexpressing cells in 48 h already been significantly low than CON cells (Fig. 3D), cell migration was also inhibited after transfection of *SPINT3* cDNA (Fig. 3E, F). These results indicated that inhibition of *SPINT3* was critical for the survival and migration of gastric cancer cell lines.

3.4 Inhibition of TGF-β1/SMAD pathway by the expression SPINT3

Considering the importance of *SPINT3* paly in gastric cancer cell proliferation and migration, we then investigate the function of *SPINT3*. *SPINT3* belong to the TGF-β1 binding pathway, even the research about *SPINT3* is limited and mainly stayed on the proteasome inhibit, we checked the rest of the genes in TGF-β1 binding pathway, take the *LTBP4* as example, it could be secreted by cultured human lung fibroblasts and stored in the ECM(extracellular matrix) either formed the complex with TGF-β1 or as a free form [16]. Deficiency of *LTBP4* would release the TGF-β1 and promote tumor metastasis [17], this inspired us to use in silico analysis to find out the mechanism of *SPINT3* induced metastasis. Firstly in the TCGA-STAD dataset, we split gastric cancer patients into ($n = 415$ total patients) *SPINT3* low expression patients ($n = 212$ patients) and *SPINT3* high expression patients ($n = 212$ patients), and calculate the up-regulated genes(adjust P value < 0.05, logFC > 1) from *SPINT3* low expression group, then using biological process in GO enrichment function, we found that the TGF-β1-related pathway was highly enriched in *SPINT3* low expression patients (Fig. 4A). We also roughly check the metastasis-related pathways including PI3K/AKT1, MEK1/GSK3β, β-Catenin and ERK1/2, results showed that most of these pathways were unchanged after *SPINT3* is overexpression in MKN-45 and MFC cell lines (Fig. 4B). On the other hand, expression of matured TGF-β1 in MKN-45 was inhibited after the transfection of *SPINT3* cDNA, along with the TGF-β1, TGF-β1 downstream component TGF-β1 type1 receptor, TGF-β1 type2 receptor, phosphorylated SMAD3(S423 + S425), total SMAD3 were all suppressed (Fig. 4C), and for the SMAD3, phosphorylated SMAD3 increased more than the total SMAD3 (Fig. 4D). Finally, we applied ELISA to detect the change of total TGF-β1 and active form of TGF-β1, and confirmed that both of them was highly increased in the supernatant of cultured medium, phenotype including MKN-45 CON, MKN-45 *SPINT3* sgRNA, MKN-45 *SPINT3* shRNA, MFC CON, MFC *Spint3* sgRNA and MFC *Spint3* shRNA cells, astonishingly that compared with sgRNA group, secretion of total and active TGF-β1 was more in the shRNA group, thus we chose shRNA phenotype for the further experiment (Fig. 4E). Combine these results together, deficiency of SPINT3 might modify the tumor microenvironment via the secretion of TGF-β1.

3.5 Modification of tumor microenvironment by knockout of SPINT3

In the previous section, we stated that knocking out or knocking down *SPINT3* could increase the secretion of TGF-β1. TGF-β1 is a well-known factor that regulates cell proliferation [18], EMT [19], and cancer metastasis [20], as well as the tumor microenvironment [21]. In the TGF-β-rich tumor microenvironment, CD8 + T cell proliferation and maturation of T helper cells are inhibited [22]. In our study, to determine the changes in immune cells in the primary tumor, we chose 615 mice owing to their immune system is normal compared with the nude mice and SCID mice we used in the Fig. 1. Firstly, we infected the MFC cell line with the CON or *SPINT3* shRNA lentivirus, and injected 5 millions of CON and *SPINT3* shRNA MFC cells into 615 mice subcutaneously. Consistent with our in vitro results, knock down of *SPINT3* increased tumor cell proliferation in vivo after 2 weeks (Fig. 5A). Then, we sort out the single cell from the primary tumor, and then labeled with different immune cell markers including LY6G, CD8A, CD45, CD11B, CD28, CD3E, LY6C, CD19, CD24, CD14, F4_80, CD326 antibodies, then samples were subjected to CyTOF analysis and clustered, visualized by TSNE, results showed that after *SPINT3* was knocked down, CD8 + CD28 + T cells decreased in number, whereas M2 macrophages, PMN-MDSCs

(CD11b^{+}Ly6G^{+}Ly6C$^{low/int}$), and MO-MDSCs (CD11b^{+}Ly6G^{-}Ly6C^{high}) increased in number (Fig. 5B, C). We further validated this change using FACS, consistent with out Cytof results, the number of CD8 + T cells was decreased (Fig. 5D) and the number of PMN-MDSCs (LY6G+) and MO-MDSCs (LY6C+) were increased(Fig. 5E). Moreover, the levels of active markers of MDSCs, including NOS2 and ARG1, significantly increased in *SPINT3* knockout tissues (Fig. 5F).

MDSCs are a bone marrow-derived heterogeneous cell population with immunosuppressive activity [23], and recent studies have shown that the expansion of MDSCs is capable of inhibiting T cell proliferation in vivo and in vitro [24]. Therefore, in our experiment, we sorted MDSCs from the primary tumors in the CON and *SPINT3* knock down groups, co-cultured them with T cells from the spleen of 615 mice, and found that the activity of the MDSCs was higher in the *SPINT3* shRNA group than in the CON group; the activity was quantified using the percentage of amplified T cells (Fig. 5G). These results suggested that, in *SPINT3* knock down primary tumors, the anti-tumor immune response was compromised, reducing cancer cell recognition and clearance, and promoting tumor cell invasion.

3.6 Blockage of SPINT3 related metastasis by reversing the expression of SPINT3 using drug treatment approach.

To block the tumor metastasis bring by *SPINT3* inhibition, we firstly trying to reverse the expression of SPINT3 by using drug treatment approach. We check the drug we have in the lab, and found that Apatinib could reverse the expression of SPINT3. Apatinib is a potent inhibitor of VEGF signaling pathway [25], which could be serve as the downstream pathway of TGF-β1 [26]. In the treatment of gastric cancer, Apatinib is a safe and effective drug for advanced gastric cancer patients [27]. As the function of SPINT3 is tightly linked to TGF-β1, we also selected TGF-β1 inhibitor SB431542 as the candidate, SB431542 is a potent and selective inhibitor of TGF-β1 type 1 receptor [28], also SB431542 could regulate the secretion of TGF-β1 in gastric [29], lung cancer cell [30].

MFC *SPINT3* shRNA cells were treated with 25 uM of Apatinib or 1 uM of SB431542 for 72 h, and using western blot, we confirmed that the expression of *SPINT3* was elevated by treatment with Apatinib and SB431542(Fig. 6A). Using Annexin FITC/PI double staining and CCK8 experiment, we also concluded that both the Apatinib and SB431542 could induce the apoptosis after 72 h of treatment, also the cell proliferation was inhibition after 48h of treatment (Fig. 6B, C), combined these results together, it's promising to use Apatinib and SB431542 to stop the SPINT3 related metastasis. So next we injected 5 million of MFC *SPINT3* shRNA cells into 615 mice subcutaneously. After 2 weeks of injection, we harvested the primary tumor from mice and digested as single cells, then using the FACS, the decreased percentage of PMN-MDSCs and MO-MDSCs were detected (Fig. 6D). We also test the function of MDSC by using the T cell proliferation assay, results showed that unlike the activated MDSCs sort from primary tumor of SPITN3 shRNA group, activation of the MDSCs from the Apatinib and SB431542 was shut down (Fig. 6E). Using the mouse model in Fig. 1A, we further proved that treatment of Apatinib and SB431542 in vivo could block the metastasis induced by SPITN3 inhibition (Fig. 6F). Combined these results

together, we concluded that the gastric cancer metastasis in SPINT3 inhibited tissue could be generally blocked by reversing the expression of SPITN3.

In summary, we discovered the model as shown in Figue 6G, in the *SPINT3* deficient tissue, secretion of TGF-β1 as elevated, which activate the function of MDSCs, and inhibit the proliferation of CD8 + T cells, these changes formed the immune suppressed TME, and finally induced tumor metastasis.

4. Discussion

In this study, we first confirmed that *SPINT3* was expressed at low levels in gastric cancer tissues and correlated it with the patient survival rate. Then, using multiple experiments, we proved that *SPINT3* expression could influence cell proliferation, migration, and apoptosis. These results show that *SPINT3* is a tumor suppressor.

The function of *SPINT3* is still unclear, and we deduced that it might be related to the TGF-β1 secretion signal as (1) *SPINT3* is involved in the TGF-β1 binding pathway, and (2) in *SPINT3* low expression gastric cancer samples, the TGF-β1 secretion and activation pathway was highly enriched (3) By using western blot, the well-known metastasis related pathway such as AKT1, MEK, GSK3β, β-catenin was not activated after *SPINT3* is inhibited. We used ELISA to detect the change in TGF-β1 concentrations in the supernatant of CON and SPINT3 sgRNA tumor cells, and found that total TGF-β1 and activated TGF-β1 levels increased. TGF-β1 has a significant impact on the recruitment, activation, and function of immune cells; in macrophages, TGF-β1 inhibits the identification and clearance of cancer cells and induces polarization from the M1 to M2 type [31], which further induces the formation of cancer-associated fibroblasts (CAFs) [32]. In NK cells, TGF-β1 can downregulate the expression of NKp30 and NKG2D on the cell surface; it can also inhibit MHC I expression in cancer cells, and suppress the function of NK cells [33]. Elevated TGF-β1 levels in the tumor microenvironment can also regulate the function of myeloid-derived cells, mainly of 3 types: (1) tumor-associated macrophages [34], (2) tumor-associated neutrophils [35], and (3) unmatured CD11B + GR1 + myeloid cells (myeloid immune suppressor cells, MISCs) or MDSCs [36]. These 3 types of cells are associated with poorer prognosis of cancer patients and resistance to target therapy. On the other hand, most of the recent studies have focused on TGF-β1 secreted by these cells, as opposed to TGF-β1 secreted by tumor cells, and on the changes in the EMT process; for example, *SALL4* overexpression in gastric cancer cells can activate TGF-β/Smad and further promote EMT, thus stimulating the metastasis of gastric cancer cells [37].

In this study, we found that the downregulation of *SPINT3* increased the number of MDSCs and M2 macrophages in the tumor microenvironment, and that the proliferation of CD8 + T cells was inhibited by the activation of MDSCs. Moreover, the upregulation of SPINT3 using drugs such as apatinib or the TGF-β1 inhibitor SB431542 could inhibit the function of MDSCs in primary tumors. Based on these results, we concluded that SPINT3 could function as a metastatic suppressor in gastric cancer through the secretion of TGF-β1.

Declarations

Conflict of interest

None

Acknowledgments

This work was supported by the Project of regional diagnosis and treatment center of health and Family Planning Commission, title is Construction of Regional Center for diagnosis and treatment of gastrointestinal cancer (NO.JBZX-201903).

Data Availability

The data used to support the findings of this study are available from the corresponding author upon request.

References

1. Zheng R, Zeng H, Zhang S, et al. Estimates of cancer incidence and mortality in China, 2013[J]. Chinese journal of cancer, 2017, 36(1): 66.
2. Oh J K, Weiderpass E. Infection and cancer: global distribution and burden of diseases[J]. Annals of global health, 2014, 80(5): 384–392.
3. Yang L, Zheng R, Wang N, et al. Incidence and mortality of stomach cancer in China, 2014[J]. Chinese Journal of Cancer Research, 2018, 30(3): 291.
4. Chen H, Lorton B, Gupta V, et al. A TGFβ-PRMT5-MEP50 axis regulates cancer cell invasion through histone H3 and H4 arginine methylation coupled transcriptional activation and repression[J]. Oncogene, 2017, 36(3): 373–386.
5. Lv L, Liu F R, Na D, et al. Transforming growth factor-β1 induces connective tissue growth factor expression and promotes peritoneal metastasis of gastric cancer[J]. Bioscience Reports, 2020, 40(9): BSR20201501.
6. Yang T, Wang R, Liu H, et al. Berberine regulates macrophage polarization through IL-4-STAT6 signaling pathway in Helicobacter pylori-induced chronic atrophic gastritis[J]. Life Sciences, 2021, 266: 118903.
7. Xiong R, Gao J, Yin T. G3BP1 activates the TGF-β/Smad signaling pathway to promote gastric cancer[J]. OncoTargets and therapy, 2019, 12: 7149.
8. Wang B, Zhao Q, Zhang Y, et al. Targeting hypoxia in the tumor microenvironment: a potential strategy to improve cancer immunotherapy[J]. Journal of Experimental & Clinical Cancer Research, 2021, 40(1): 1–16.
9. Clauss A, Persson M, Lilja H, et al. Three genes expressing Kunitz domains in the epididymis are related to genes of WFDC-type protease inhibitors and semen coagulum proteins in spite of lacking

similarity between their protein products[J]. BMC biochemistry, 2011, 12(1): 1–13.

10. Robertson I B, Rifkin D B. Regulation of the bioavailability of TGF-β and TGF-β-related proteins[J]. Cold Spring Harbor Perspectives in Biology, 2016, 8(6): a021907.
11. Zhou Y, Koli K, Hagood J S, et al. Latent transforming growth factor-β-binding protein-4 regulates transforming growth factor-β1 bioavailability for activation by fibrogenic lung fibroblasts in response to bleomycin[J]. The American journal of pathology, 2009, 174(1): 21–33.
12. Chen W, Wang Q, Xu X, et al. Vasorin/ATIA promotes cigarette smoke–induced transformation of human bronchial epithelial cells by suppressing autophagy-mediated apoptosis[J]. Translational oncology, 2020, 13(1): 32–41.
13. Man J, Yu X, Huang H, et al. Hypoxic induction of vasorin regulates Notch1 turnover to maintain glioma stem-like cells[J]. Cell stem cell, 2018, 22(1): 104–118. e6.
14. Yoon J H, Choi S S, Kim O, et al. Inactivation of NKX6. 3 in the stomach leads to abnormal expression of CDX2 and SOX2 required for gastric-to-intestinal transdifferentiation[J]. Modern Pathology, 2016, 29(2): 194–208.
15. Yu H, Wei W, Cao W, et al. Regulation of cell proliferation and metastasis by microRNA-593-5p in human gastric cancer[J]. OncoTargets and therapy, 2018, 11: 7429.
16. Koli K, Hyytiäinen M, Ryynänen M J, et al. Sequential deposition of latent TGF-β binding proteins (LTBPs) during formation of the extracellular matrix in human lung fibroblasts[J]. Experimental cell research, 2005, 310(2): 370–382.
17. Yang X, Ye X, Zhang L, et al. Disruption of LTBP4 Induced Activated TGFβ1, Immunosuppression Signal and Promoted Pulmonary Metastasis in Hepatocellular Carcinoma[J]. OncoTargets and therapy, 2020, 13: 7007.
18. Tang X, Tu G, Yang G, et al. Autocrine TGF-β1/miR-200s/miR-221/DNMT3B regulatory loop maintains CAF status to fuel breast cancer cell proliferation[J]. Cancer letters, 2019, 452: 79–89.
19. Pezone A, Taddei M L, Tramontano A, et al. Targeted DNA oxidation by LSD1–SMAD2/3 primes TGF-β1/EMT genes for activation or repression[J]. Nucleic acids research, 2020, 48(16): 8943–8958.
20. Li T, Huang H, Shi G, et al. TGF-β1-SOX9 axis-inducible COL10A1 promotes invasion and metastasis in gastric cancer via epithelial-to-mesenchymal transition[J]. Cell death & disease, 2018, 9(9): 1–18.
21. Liu Q, Wu H, Li Y, et al. Combined blockade of TGf-β1 and GM-CSF improves chemotherapeutic effects for pancreatic cancer by modulating tumor microenvironment[J]. Cancer Immunology, Immunotherapy, 2020, 69(8): 1477–1492.
22. Dahmani A, Delisle J S. TGF-β in T cell biology: Implications for cancer immunotherapy[J]. Cancers, 2018, 10(6): 194.
23. Groth C, Hu X, Weber R, et al. Immunosuppression mediated by myeloid-derived suppressor cells (MDSCs) during tumour progression[J]. British journal of cancer, 2019, 120(1): 16–25.
24. Joyce D, Fujino M, Morita M, et al. Induced pluripotent stem cells-derived myeloid-derived suppressor cells regulate the CD8 + T cell response[J]. Stem cell research, 2018, 29: 32–41.

25. Lin Y, Zhai E, Liao B, et al. Autocrine VEGF signaling promotes cell proliferation through a PLC-dependent pathway and modulates Apatinib treatment efficacy in gastric cancer[J]. Oncotarget, 2017, 8(7): 11990.
26. Sun H, Miao C, Liu W, et al. TGF-β1/TβRII/Smad3 signaling pathway promotes VEGF expression in oral squamous cell carcinoma tumor-associated macrophages[J]. Biochemical and biophysical research communications, 2018, 497(2): 583–590.
27. Zhang Y, Han C, Li J, et al. Efficacy and safety for Apatinib treatment in advanced gastric cancer: a real world study[J]. Scientific reports, 2017, 7(1): 1–9.
28. Alyoussef A. Blocking TGF-β type 1 receptor partially reversed skin tissue damage in experimentally induced atopic dermatitis in mice[J]. Cytokine, 2018, 106: 45–53.
29. Liu X S, Lin X K, Mei Y, et al. Regulatory T cells promote overexpression of Lgr5 on gastric cancer cells via TGF-beta1 and confer poor prognosis in gastric cancer[J]. Frontiers in immunology, 2019, 10: 1741.
30. Liao K, Yong C W, Hua K. SB431542 inhibited cigarette smoke extract induced invasiveness of A549 cells via the TGF β1/Smad2/MMP3 pathway[J]. Oncology letters, 2018, 15(6): 9681–9686.
31. Jayaraman P, Parikh F, Newton J M, et al. TGF-β1 programmed myeloid-derived suppressor cells (MDSC) acquire immune-stimulating and tumor killing activity capable of rejecting established tumors in combination with radiotherapy[J]. Oncoimmunology, 2018, 7(10): e1490853.
32. Liu F L, Mo E P, Yang L, et al. Autophagy is involved in TGF-β1-induced protective mechanisms and formation of cancer-associated fibroblasts phenotype in tumor microenvironment[J]. Oncotarget, 2016, 7(4): 4122.
33. Han B, Mao F, Zhao Y, et al. Altered NKp30, NKp46, NKG2D, and DNAM-1 expression on circulating NK cells is associated with tumor progression in human gastric cancer[J]. Journal of immunology research, 2018, 2018.
34. Zhang D, Qiu X, Li J, et al. TGF-β secreted by tumor-associated macrophages promotes proliferation and invasion of colorectal cancer via miR-34a-VEGF axis[J]. Cell Cycle, 2018, 17(24): 2766–2778.
35. Lianyuan T, Gang L, Ming T, et al. Tumor associated neutrophils promote the metastasis of pancreatic ductal adenocarcinoma[J]. Cancer Biology & Therapy, 2020, 21(10): 937–945.
36. Zhang C, Zhang Y, Zhang W, et al. WISP1 promotes bovine MDSC differentiation via recruitment of ANXA1 for the regulation of the TGF-β signalling pathway[J]. Molecular and Cellular Biochemistry, 2020, 470: 215–227.
37. Ma Y, Xue H, Wang W, et al. The miR-567/RPL15/TGF-beta/Smad axis inhibits the stem-like properties and chemo-resistance of gastric cancer cells[J]. TRANSLATIONAL CANCER RESEARCH, 2020, 9(5): 3539–3549.

Tables

Table 1 is available in the Supplementary Files section.

Figures

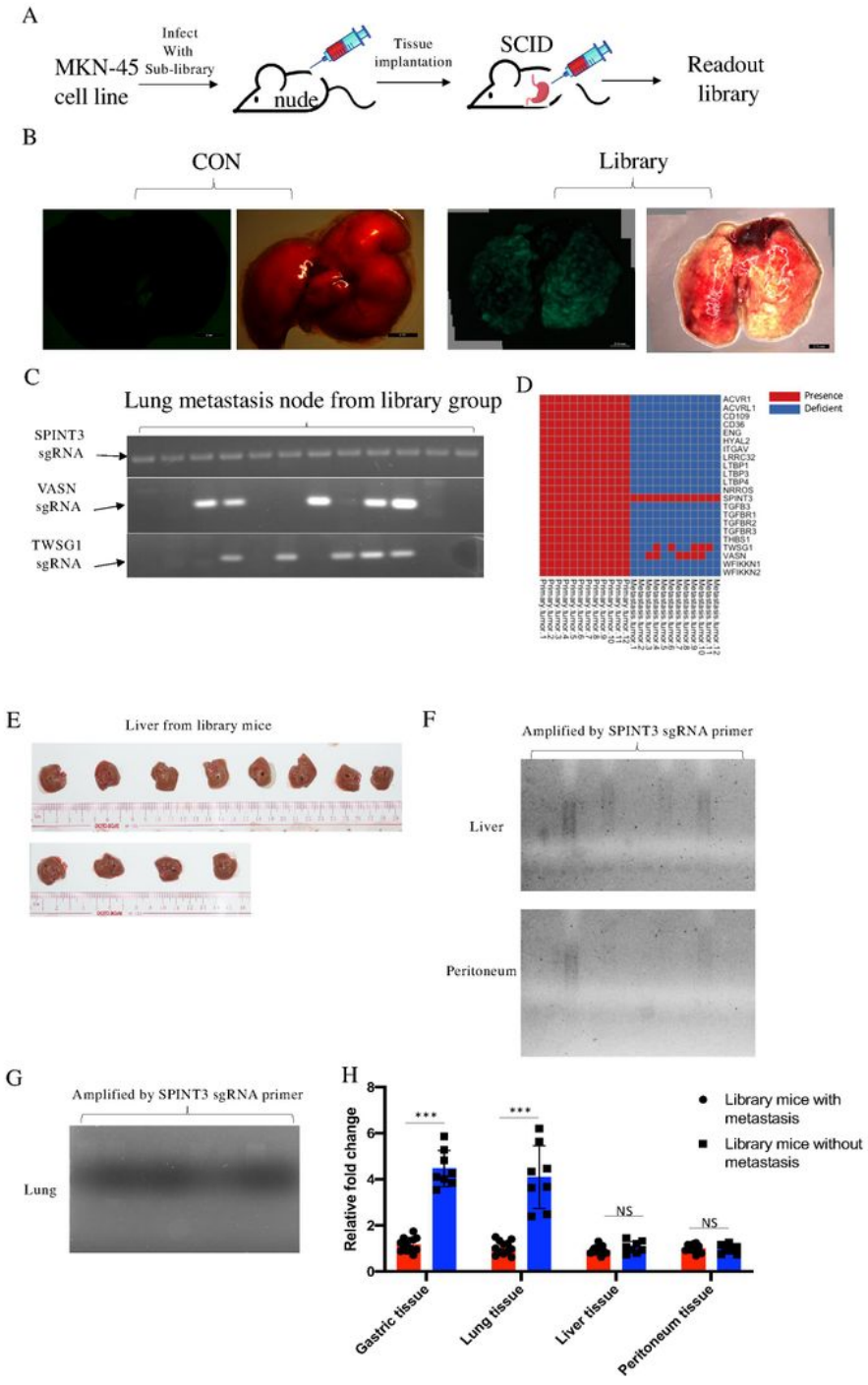

Figure 1

Identification of SPINT3 as a possible metastatic suppressor by using CRISPR knock out sub-library

(1) Pipeline of implantation of gastric cancer tissue (*n* = 12 mice). (B) SCID mice which implant with gastric cancer tissue were dissected, and using fluorescence microscope to detect the GFP intensity in lung (*n* = 12 mice). (C) Genome DNA from lung were extracted, and amplified by SPINT3, VASN and TWSG1 sgRNA specific primer (*n* = 12 mice). (D) Presence of 22 sgRNAs in all the primary tumor and metastatic tumor tissue (*n* = 12 mice). (E) Plot of the liver from library mice which had lung metastatic tumor (*n* = 12 mice). (F) Genome DNA of livers and peritoneums from library mice which had lung metastatic tumor were extracted, then amplified by SPINT3 sgRNA specific primer (*n* = 12 mice). (G) Genome DNA of lungs from library mice without metastatic tumor were extracted, then amplified by SPINT3 sgRNA specific primer (*n* = 8 mice). (H) Expression of SPINT3 in mRNA level in gastric tissue, lung tissue, liver tissue and peritoneum and tissue from library mice which had lung metastatic tumor (*n* = 12 mice) and without lung metastatic tumor (*n* = 8 mice) were quantified by QPCR. Error bars in this mean ± SD. 2-tailed Student's t test was used to calculate significance. ***$P < 0.001$, NS means there was no statistical significance.

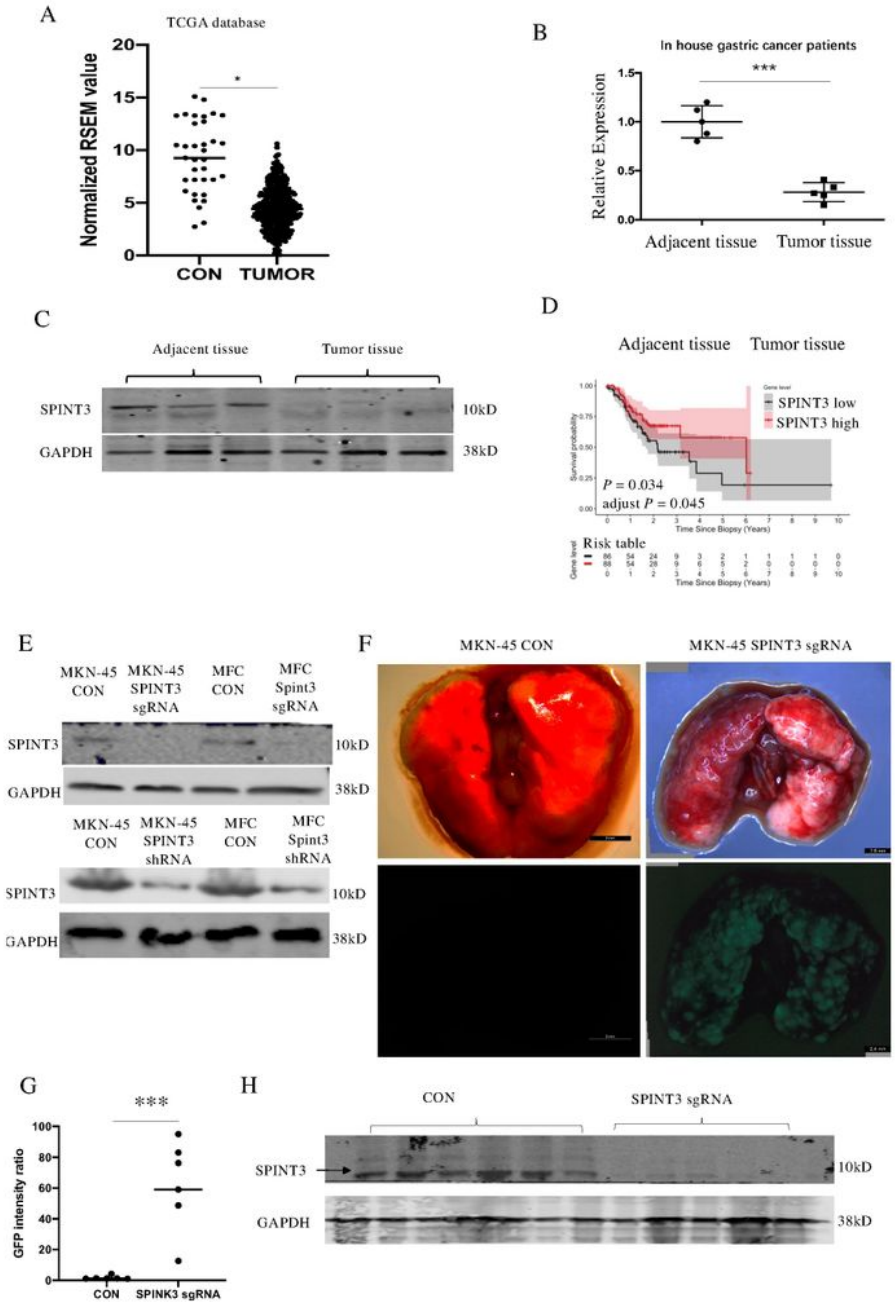

Figure 2

Deficiency of SPINT3 increased lung metastasis of gastric cancer cell line.

(A) In TCGA-STAD dataset, RSEM value of healthy donor (*n* = 35) gastric cancer tumor (*n* = 415) were extracted, the normalized by log2 transformation. (B) From our in-house data, using QPCR to detect expression of SPINT3 in 5 cases of gastric cancer tissue and adjacent tissue in mRNA level. (C) Using

western blot to detect expression of SPINT3 in 6 cases of gastric cancer tissue and adjacent tissue in protein level. (D) In TCGA-STAD dataset, using univariate COX analysis to detect relation of SPINT3 expression and patients' prognosis (n = 174 patients). (E) Gastric cancer cell line MKN-45 and MFC were infected with CON, SPINT3 sgRNA and SPINT3 shRNA for 48h, then using western blot to detect the change of SPINT3 expression in protein level (n = 3/group). (F) Metastasis ability of CON and SPINT3 sgRNA cells were detected by the mouse model in Figure 1A (n = 6 mice/group). (G) GFP intensity in CON and SPINT3 sgRNA were detected by image J software (n = 6 mice/group). (H) Using western blot to detect the change of SPINT3 in CON and SPINT3 sgRNA (n = 6 mice/group). Error bars in this mean ± SD. 2-tailed Student's t test was used to calculate significance. *P < 0.05, ***P < 0.001.

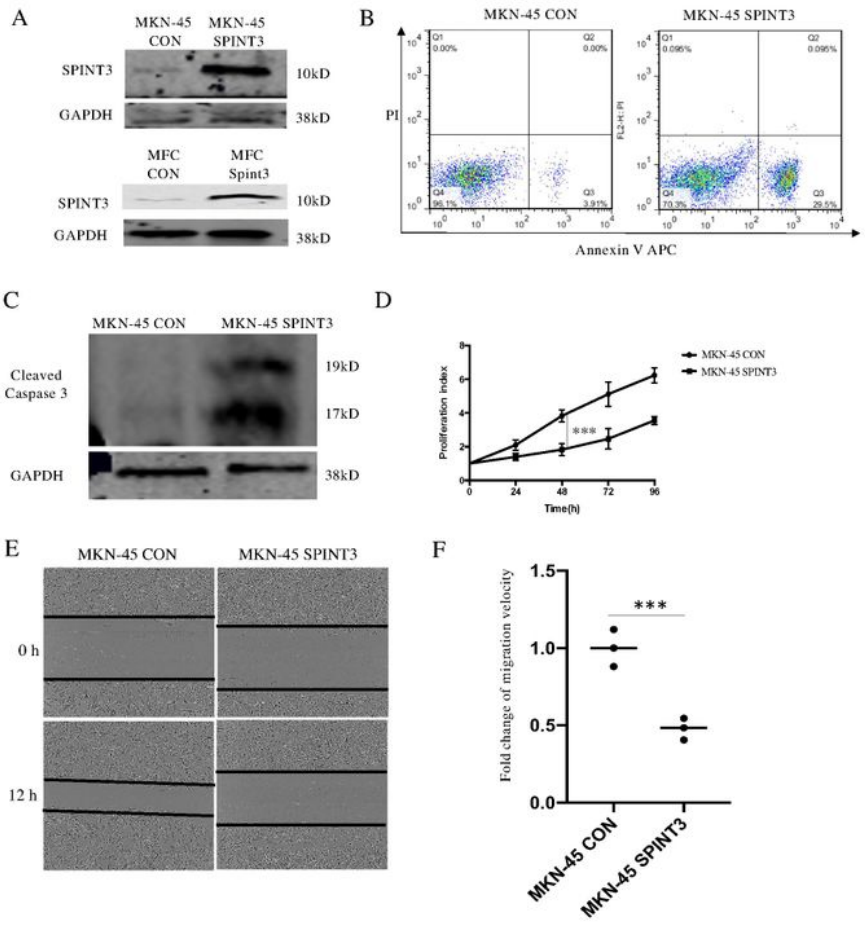

Figure 3

Relation between expression of SPINT3 and biological characteristics of gastric cancer cell.

Gastric cancer cells MKN-45 and MFC were divided into CON and SPINT3 group, then transfected with CON and SPINT3 cDNA, after 48h. (A) Using western blot to detect the change of expression of SPINT3 in MKN-45 CON, MKN-45 SPINT3 (upper panel) and MFC CON, MFC SPINT3 (lower panel) in protein level.

(B) Using Annexin V APC/PI double staining to detect the change of cell apoptosis. (C) Using western blot to detect the change of cleaved caspase3 in protein level. (D) Using CCK8 to detect the change of cell proliferation. (E) Using wound healing assay to detect the change of cell migration. (F) Summary of fold change the velocity of migration in (D). All the experiment above were replicated by 3 times. Error bars in this mean ± SD. 2-tailed Student's t test was used to calculate significance. ***$P < 0.001$.

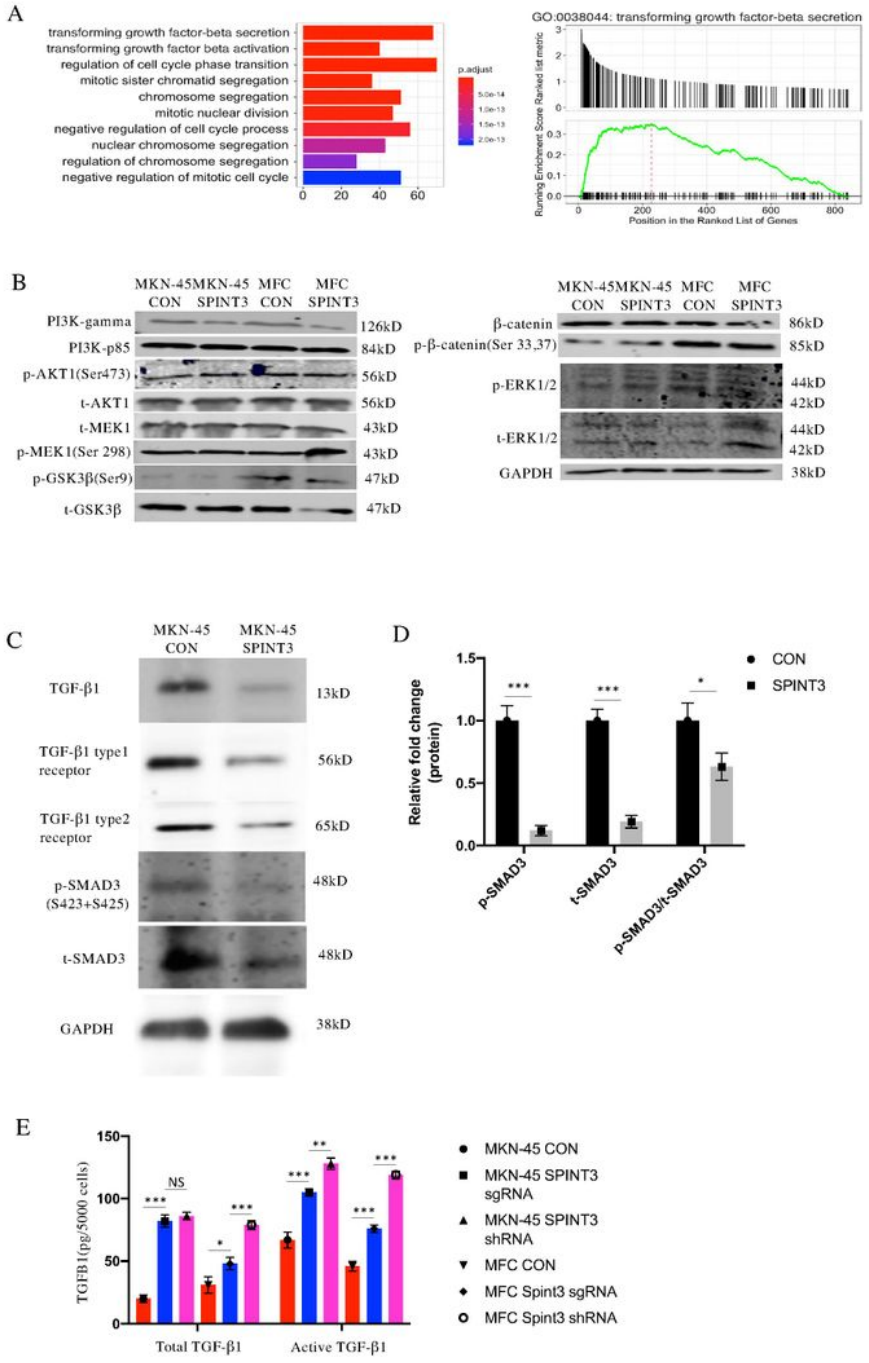

Figure 4

Inhibition of TGF-β1/SMAD pathway by SPINT3

(A) In TCGA database, samples were divided into SPINT3 low and high expression group, then detect pathway enrichment in SPINT3 low expression group. (B) Using western blot to detect the change of PI3K-gamma, PI3K-p85, phosphorylated AKT1(Ser473), total AKT1, total MEK1, phosphorylated MEK1, phosphorylated GSK3β(Ser9), total GSK3β, β-catenin, phosphorylated β-catenin (Ser 33,37), phosphorylated ERK1/2 and t-ERK in MKN-45 CON, MKN-45 SPINT3, MFC CON and MFC SPINT3 in protein level. (C) Using western to detect the change of TGF-β1/SMAD3 pathway including matured TGF-β1, TGF-β1 type1 receptor, TGF-β1 type2 receptor, p-SMAD3(S423+S425), total SMAD3 in protein level. (D) Gray value of phosphorylated SMAD3(S423+S425) and total SMAD3 were calculated by Image J software, then using the relatively fold change to quantify the change of phosphorylated SMAD3(S423+S425) and total SMAD3. (E) Using ELISA to determine total TGF-B1 and active TGF-B1 in the supernatant of MKN-45 CON, MKN-45 SPINT3-shRNA, MKN-45 SPINT3 sgRNA, MFC CON, MFC SPINT3-shRNA and MFC SPINT3 sgRNA cells. All the experiment above were replicated by 3 times. Error bars in this mean ± SD. 2-tailed Student's t test was used to calculate significance. $*P < 0.05$, $***P < 0.001$, NS means there was no statistical significance.

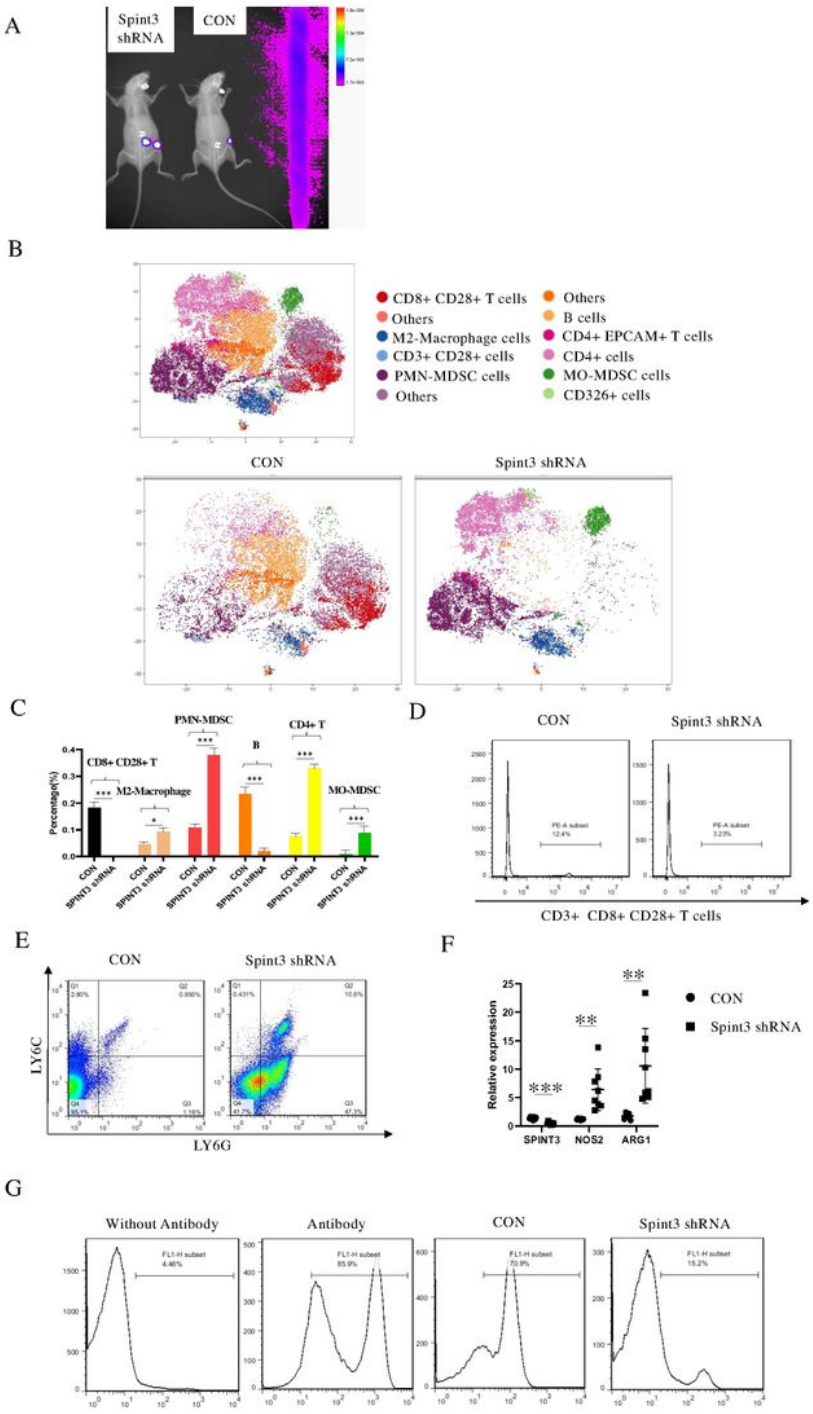

Figure 5

Modification of tumor microenvironment by knockout of SPINT3

(A) 5 million of CON and SPINT3 shRNA MFC cells were injected in 615 mice subcutaneous, after 2 weeks of injection, IVIS® Spectrum In Vivo Imaging System was used to detect the tumor cell proliferation in vivo (*n* = 7 mice/group). (B) Primary tumor from (A) were harvested, then the single cell were sorted, and

the change of immune cell component were analyzed by Cytof (*n* = 7 mice/group). (C) Summary figure of the change of immune cells in CD45+ cells. Percentage of CD8+ T cell(E) and MDSCs (*n* = 7 samples/group). (D) Percentage of CD3+ CD8+ CD28+ T cells and (E) MDSCs in the primary tumor of (A) were further validated by FACS (*n* = 7 samples/group). (F) CD11B+ GR1+ cells from primary tumor were sort out by FACS, and using QPCR to detect the change of SPINT3, NOS2 and ARG1 (*n* = 7 samples/group). (G) MDSCs from CON and SPINT3 sgRNA primary tumor were co-cultured with T cells from spleen, and using CFSE to detect the change of cell proliferation (*n* = 7 samples/group). Error bars in this mean ± SD. 2-tailed Student's t test was used to calculate significance. **P* < 0.05, ***P* < 0.01, ****P* < 0.001.

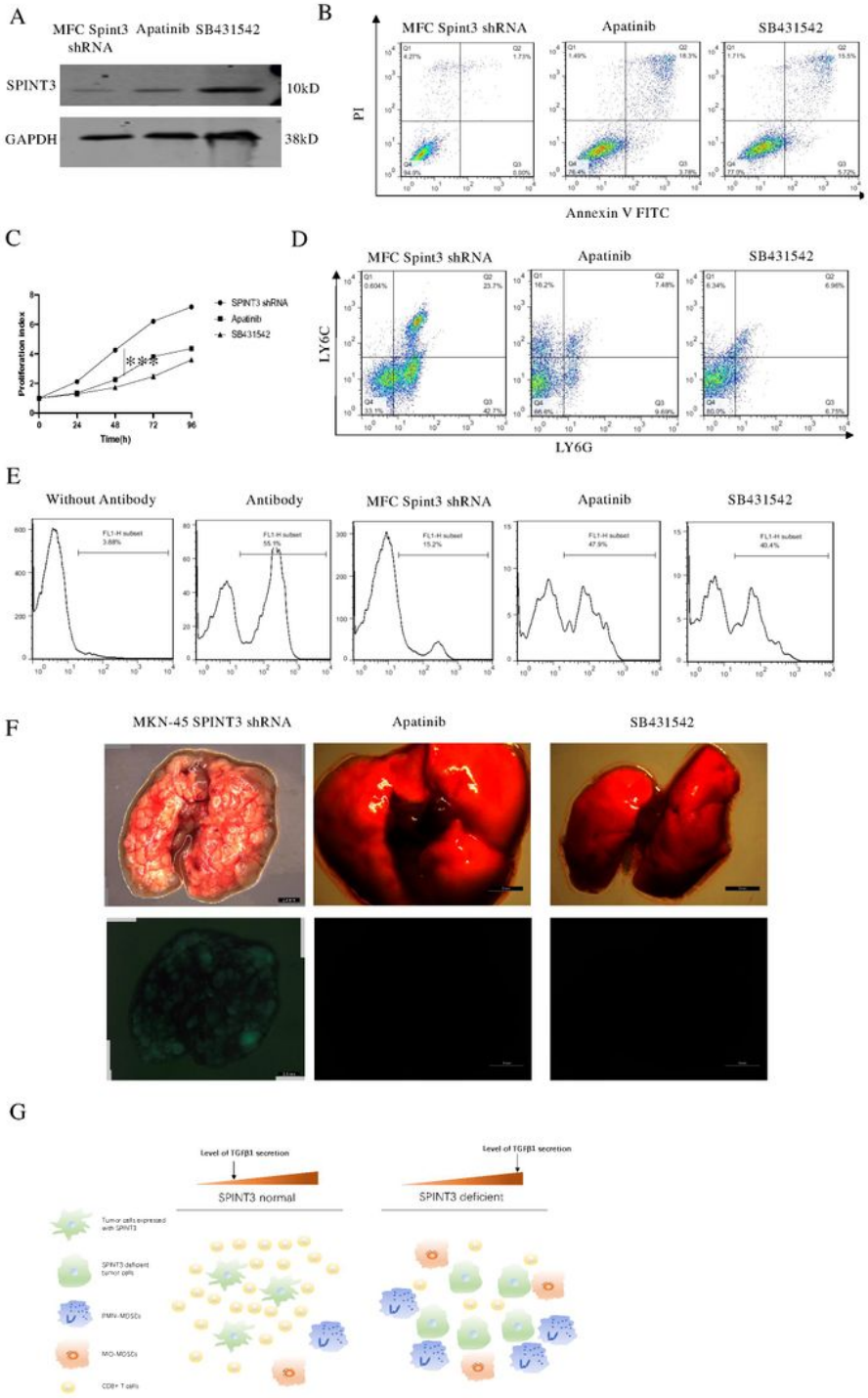

Figure 6

Blockage of SPINT3 related metastasis by reversing the expression of SPINT3 using drug treatment approach.

(A) MFC SPINT3 shRNA were treated with 25 uM of Apatinib or 1 uM of SB431542 for 72 h, and using western blot to detect the change of SPINT3 in protein level. (B)Employing Annexin V/PI to measure the

change of cell apoptosis in MFC SPINT3 shRNA, Apatinib and SB431542 group. (C) Using CCK8 to measure the change of cell proliferation in MFC SPINT3 shRNA, Apatinib and SB431542 group. (D) 615 mice were firstly injected with 5 million of MFC SPINT3 shRNA cells in 615 mice subcutaneous, and then divided into MFC SPINT3 shRNA, Apatinib and SB431542 group, after 3 days of injection, MFC SPINT3 shRNA were injected with 100 uL of PBS intraperitoneal, Apatinib group were injected with 50 mg/kg of Apatinib intraperitoneal 2 times a week, SB431542 group were injected with 100 uL of SB431542 (1uM solution) intraperitoneal 2 times a week. After 2 weeks of injection, primary tumor of 3 groups were harvested, and using FACS to detect the percentage of PMN-MDSC and MO-MDSC in MFC SPINT3 shRNA, Apatinib and SB431542 group. (E) T cells from the bone marrow of 615 were sorted out by FACS, then mix with the MDSCs from the primary tumor of mice in (D), and using CFSE to detect the change of T cell proliferation. (F) MKN-45 cell line were infected with CON or SPINT3 shRNA lenti virus for 48 h, then applied the mouse model as Figure 1A descripted, then mice were treated with Apatinib or SB431542 as (D) descripted, then the tumor metastasis in each group were detected. (G) Summary figure the whole research.

Supplementary Files

This is a list of supplementary files associated with this preprint. Click to download.

- Genenameof22genelibrarylist.xls
- fulllengthgelafterrevise.pdf